

The electronic side of the double-layer: Impact on diagnostics and improvement of carbon double layer electrodes.

R. Kötz, M. Hahn, O. Barbieri, J.-C. Sauter, R. Gallay*

Paul Scherrer Institut, CH-5232 Villigen, Switzerland

* Maxwell Technologies SA, CH-1728 Rossens, Switzerland

Introduction

In order to bring supercapacitors to the market and make them an indispensable element among energy storage devices, manufacturers and developers try to improve the performance of supercapacitors in terms of energy and power density. One measure toward a better performance is the increase of the nominal voltage U of the supercapacitor. As U^2 affects both energy and power the increase of the available potential window would be a very effective step.

In addition an increased capacitance will also improve the energy density. Larger capacitance can be achieved by an increased specific surface area of the active material as well as by an increased specific double layer capacitance.

Taking a typical value of the double layer capacitance (DLC) of a metal, 20 - 30 $\mu\text{F}/\text{cm}^2$, and a surface area of activated carbon of 2000 m^2/g a specific capacitance of 400 - 600 F/g should be achievable. Typical values achieved today, however are around 100 F/g when using organic electrolytes. Several authors investigated reasons for the relatively small specific capacitance of today's real supercapacitor electrodes in non-aqueous electrolytes. It was found that the specific double layer capacitance may be significantly smaller than expected /1/ and that part of the BET surface area is not accessible to the electrolyte, because the pore size distribution may not match the size of the available anions or cations /2/.

In fact, available data for the double layer capacitance of various carbons vary between 1 and 100 $\mu\text{F}/\text{cm}^2$. For activated carbons a DLC was reported between 5 and 20 $\mu\text{F}/\text{cm}^2$ when related to the measured BET surface area of the respective carbon /3/. Similar values were reported also for organic, aprotic electrolytes /4, 5/. In order to fit the experimental data for activated carbon fibers in aqueous electrolyte Shi /1/ assumed a DLC of 14.5 $\mu\text{F}/\text{cm}^2$ for micropores and a DLC of 7.5 $\mu\text{F}/\text{cm}^2$ for external surface.

In contrast to an ideal capacitor with a constant capacitance independent of the state of charge, a typical electrochemical double layer capacitor exhibits a potential dependent capacitance. In addition to the absolute number of the DLC of activated carbons the potential dependence of the DLC is of significant importance for the performance of a double layer capacitor. Cyclic voltammograms for carbon based double layer capacitor electrodes measured by various authors exhibit a pronounced potential dependence of the capacitance,

which has been explained by the presence of surface functional groups (especially in aqueous electrolytes) or other pseudo capacitance, or by a potential dependent accessibility of pores.

In the present contribution we report about simultaneous *in situ* measurements of the potential dependent capacitance of a real AC based double layer electrode in organic electrolyte and of the potential dependent electronic conductance of the very same electrode /6/.

Experimental

The electrode material used was a commercial PTFE-bound activated carbon with a BET-surface of 1050 m²/g. A solution of 1 mol/l Et₄NBF₄ in acetonitrile was employed as the electrolyte.

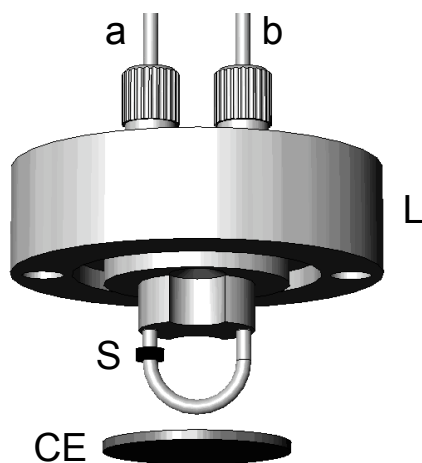


Fig. 1: 3-D view of the electrode arrangement in the measuring cell. The counter electrode (CE) is mounted at the bottom of an electrolyte container (not shown). The sample (S) is clamped between two gold wires (a, b). After assembling the cell is filled with the electrolyte solution through an additional opening in the lid (L).

The cover of the electrochemical cell with integrated sample holder is shown in Figure 1. Its essential part consists of two gold wires clamping a small electrode sample (2 mm in diameter, 0.6 mm thick). The sample is immersed into the electrolyte solution, and stepwise electrochemically charged against a counter electrode made from the same material and placed below the sample on the bottom of the electrolyte container. Since the counter electrode is much larger than the sample, its potential is effectively pinned upon charging. Thus the electrode potential, U , can be directly recorded with respect to the counter electrode, whose potential is considered to be the pzc.

At each potential step both, the electronic conductance across the sample and the electrochemical impedance between the sample and the counter electrode are measured.

The electronic conductance, $L = i/U_{ab}$, is determined by applying a small dc-current, i , across the sample and measuring the corresponding potential drop, U_{ab} (some mV), between the two wires (a and b in Fig. 1).

The capacitance, C , is calculated from the imaginary part, Z^{im} , of the electrochemical impedance at a frequency $f = 10$ mHz, according to $C = -1/(2\pi f Z^{im})$.

Results and Discussion

The cyclic voltammogram of a single commercial PTFE-bound activated carbon based double layer capacitor electrode in 1M Et_4NBF_4 in acetonitrile is shown in figure 2a. The potential is referenced versus the potential of zero charge. The CV exhibits a clear “butterfly” shape with a capacitance minimum at the pzc and increasing capacitance toward positive and negative charging.

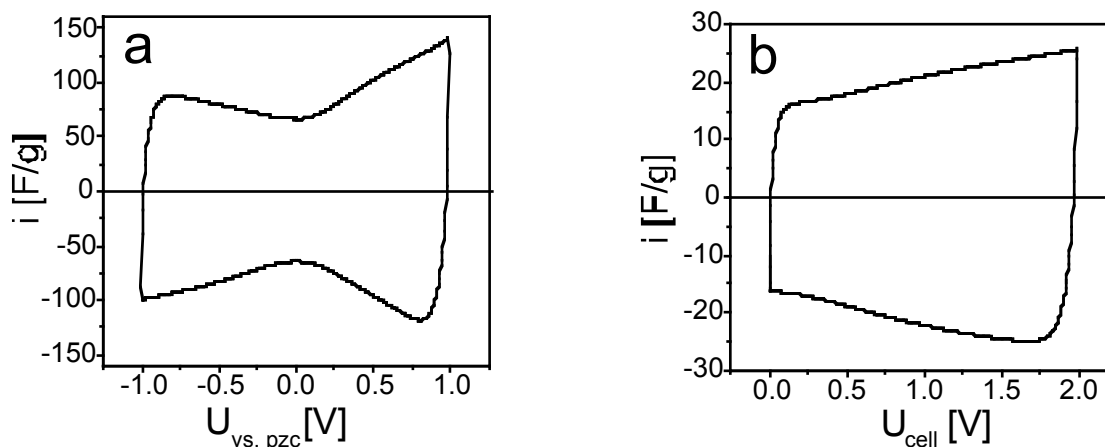


Fig. 2 (a) Cyclic voltammogram of a single activated carbon electrode. The measuring device used is shown in Fig. 1. (b) Cyclic voltammogram of the complete DLC device, consisting of two equal-sized electrodes. For both diagrams, the current is normalized to the dry carbon mass of the single electrode and of the device, respectively, and the sweep rate of 10 mV/s. Electrolyte: 1 mol/l Et_4NBF_4 in acetonitrile.

The fact that the shape of the CV is nearly symmetrical around the pzc indicates that the pore structure of the material is designed for anion as well as cation transport. The consequence of such an electrode characteristic for the capacitor performance is demonstrated in figure 1b, where the CV of the 2-electrode arrangement of the above electrode material is shown. The specific capacitance of the capacitor is 1/4 of the capacitance of the single electrode and increases from the discharged state towards the charged state by almost a factor of 2. This behavior is also observed for commercial capacitors during constant current

charge/discharge tests. During such tests the slope of the potential increase/decrease is smallest in the charged state.

Figure 3 shows the capacitance together with the electronic conductance of the single electrode as a function of the electrode potential. The capacitance was determined from the impedance measurement according to $C = 1 / (2 \pi \omega Z_{\text{imag}})$ and normalized with respect to the BET surface area, which was $1050 \text{ m}^2/\text{g}$. The conductance is normalized to be 1 at the pzc. Both capacitance and conductance have a very similar dependence on the electrode potential with a pronounced minimum close to the pzc.

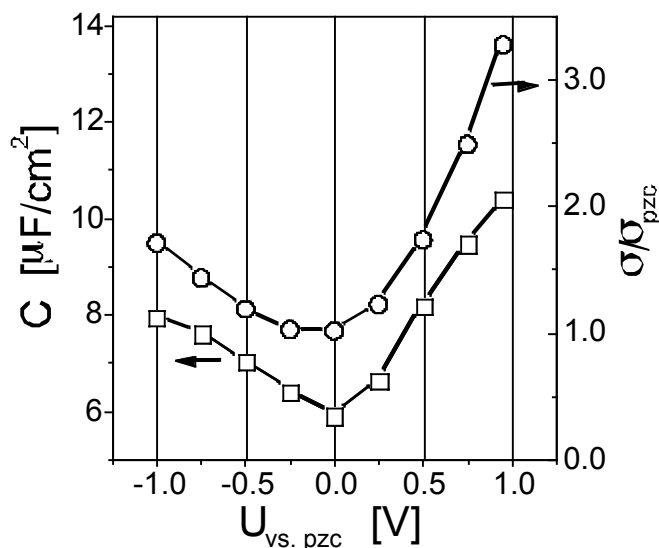


Fig. 3 Capacity (squares) and normalized electronic conductance (circles) vs. electrode potential. $\sigma_{\text{pzc}} = 500 \text{ S/m}$. Stepwise charging (0.25 V and 600 s per step). Only the data of one positive potential sweep are shown. C is calculated from the electrochemical impedance measured at 10 mHz. The measuring device used is depicted in Fig. 1. Electrolyte: 1 mol/l Et_4NBF_4 in acetonitrile. Drawn lines connect the measured data points and are a guideline to the eye.

Conductivity

For a metal-like conductor with a finite density of states at the Fermi level, $D(E_F)$, the conductivity may be described by [7]

$$\sigma = e_0 \mu(E_F) D(E_F) kT \quad (1)$$

where $\mu(E_F)$ is the mobility, assigned to the electronic states at the Fermi level. It is obvious from (1) that the density of states and the mobility affect the

conductivity. Assuming the mobility is constant, only changes in D may be responsible for the measured dependence on the electrode potential. The applied electrode potential will affect D only in a narrow surface layer of the carbon electrode, characterized by the screening length (Fermi length) of the electric field inside the metal-like pore walls,

$$\delta_{SC} = \sqrt{\frac{\epsilon \epsilon_0}{e_0^2 D(E_F)}} \quad (2)$$

where ϵ is the relative dielectric constant in the direction normal to the graphene layers, ϵ_0 is the vacuum permittivity, and e_0 is the absolute value of the electronic charge.

Consequently, only if δ_{SC} is comparable to the thickness of the pore walls, the electrode potential is expected to affect the conductivity. Obviously, this assumption is fulfilled for the highly porous electrode material, where the thickness of the pore walls can be estimated to be some graphene layers only.

The potential variation at a pore wall is sketched in Figure 4. The potential difference between pore electrolyte and electrode (pore wall) is distributed between the electrolyte side (Helmholtz layer) and the electrode side (space charge layer). According to the potential variations within the solid, electronic states are filled/emptied and the conductance varies consequently.

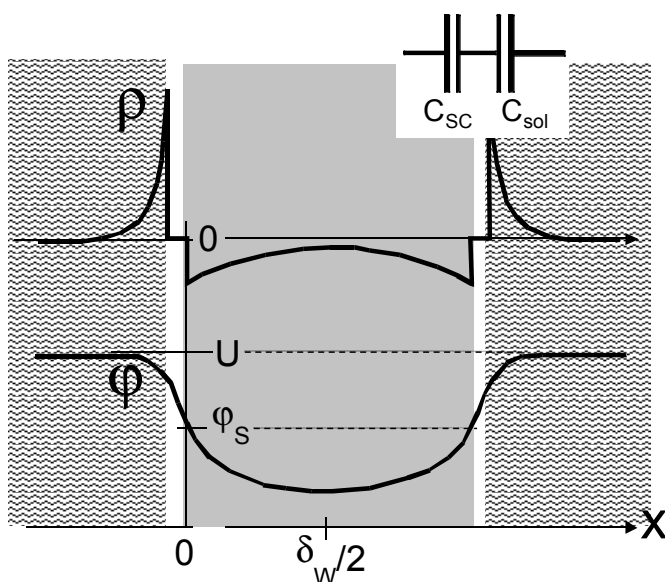


Fig. 4 Sketch of charge and potential distribution across the pore wall and the adjacent solution phase inside the pores. The inset shows the equivalent circuit used to separate the space charge capacitance, C_{SC} , from the overall capacitance, C_{tot} .

We therefore assume that the density of states (DOS) and thus the conductance at the surface of the carbon pore walls is affected by the electrode potential,

which shifts the position of the Fermi level. A shift of the Fermi level results in a change of D .

Capacitance

If part of the potential drop is located within the solid as shown in figure 4 it becomes evident that the interface capacitance can be divided into two contributions, one on the electrolyte side and one on the solid side, both being connected in series. The smaller of these capacitances will dominate the overall interface capacitance. E.B. Yeager and also H. Gerischer have addressed this problem of a possible space charge contribution to the interface capacitance of graphite in depth before.

Treating HOPG as a narrow gap semiconductor, with the charge carriers obeying Boltzmann statistics, Yeager calculated a space charge capacity, C_{sc} , being nearly identical with the measured capacity minimum at the pzc [8, 9]. Thus, almost the whole potential drop across the double layer must be attributed to the space charge layer inside the solid. In a thorough re-examination of Yeager's experimental data, Gerischer confirmed this conclusion [10]. However, he argued that HOPG must be treated more appropriately as a metal with a low, but still finite density of states at the Fermi level, $D(E_F)$. Then, for a constant density of states, C_{sc} is given by

$$C_{sc} = e_0 \sqrt{\epsilon \epsilon_0 D(E_F)} \quad (3)$$

According to the above considerations, it is clear that conductance as well as capacitance of the carbon electrolyte interface may be affected by the potential applied provided the density of states D is such that the screening length of the field within the solid is at least comparable to that on the electrolyte side. In addition, for the conductance to be affected the extension of the space charge region has to be comparable to the thickness of the pore wall.

Using a computational fitting program the measured conductance was fitted by calculating the respective distribution of the density of states (DOS), which are filled/emptied during electrochemical charging/discharging. As is evident in figure 5 results for both the conductance as well as for the capacitance can be well reproduced with a common density of states distribution.

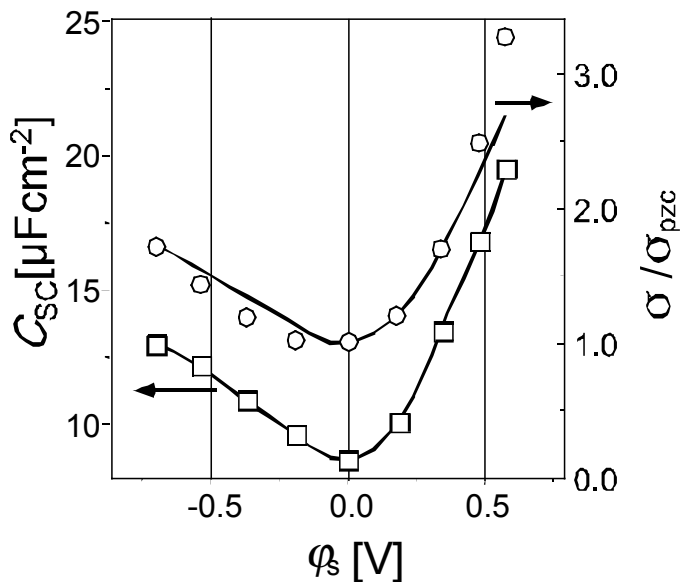


Fig. 5 Space charge capacity (black) and conductivity (blue) as a function of ϕ_s (taking $C_{sol} = 30 \mu\text{F}/\text{cm}^2$). Symbols indicate measured values, lines indicate fit of capacity by DOS, and conductivity calculated subsequently according to eq. (3), respectively.

DOS distributions for graphite and HOPG were determined before [11,12] and are reproduced in figure 6 together with the present results.

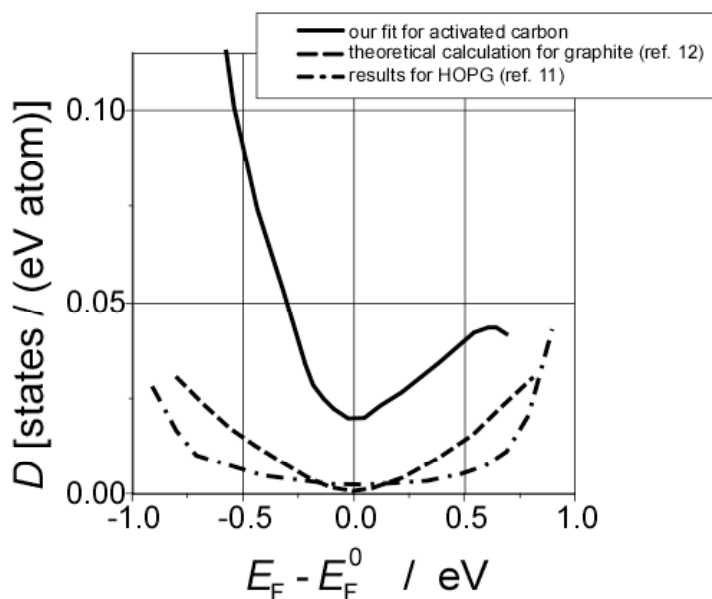


Fig. 6 DOS of activated carbon (our fit result) compared to two previous results for graphite [11, 12]. The dos is given as a function of the shift of the Fermi level with respect to the uncharged state, $E_F - E_F^0$.

While the approach of Gerischer was adapted in the present investigation we extended this approach by measuring the electronic conductance simultaneously. The fact that both quantities can be explained by the same assumption substantiates the approaches discussed earlier by Gerischer and Yeager.

The DOS result of our investigation was found to be significantly higher than previous calculations for graphite and HOPG. This may be due to the fact that we

investigated activated carbon with a significant number of defects and grain boundaries.

Implications for Capacitors and Conclusions

The above results were obtained on a commercial capacitor electrode and may well be a result of the special carbon or the chosen electrolyte. In order to investigate the validity of the measured potential dependence we have investigated different electrolytes as well as different carbons.

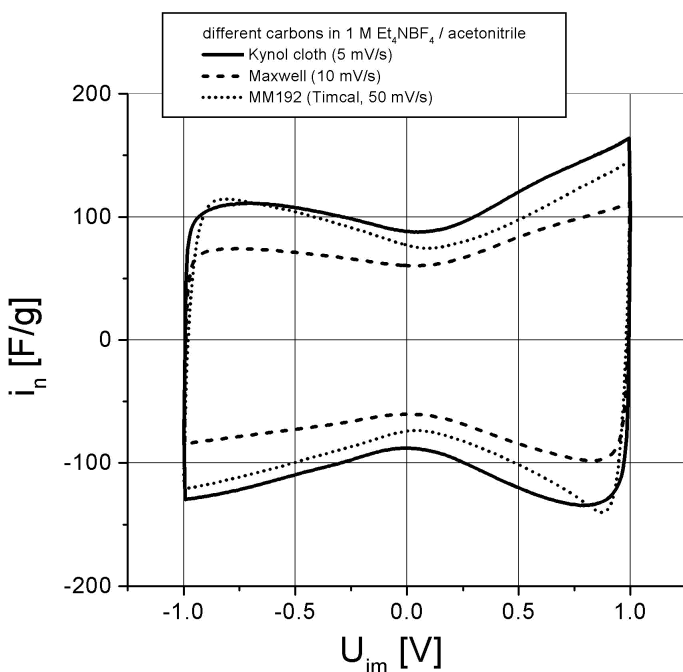


Fig. 7 Cyclic voltammogram (current recalculated to obtain specific capacitance) of different carbons (commercial electrode, Kynol fiber cloth and TIMCAL activated carbon MM192) in organic electrolyte

The behavior of different carbons is reproduced in figure 7. As a result it is obvious that the type of carbon does not change the effect of the electrode potential on the capacitance. For all carbons the typical butterfly shape is observed. This confirms our general assumption that the variation of the charge carrier density in the carbon is responsible for the observed effect.

Figure 8 shows the cyclic voltammogram of one and the same electrode (Kynol AC Fibers) in organic as well as in aqueous electrolyte. While the well-known butterfly shape is obtained for this carbon in the organic electrolyte a totally different potential dependence of the capacitance is observed for the aqueous acidic electrolyte. In contrast to the organic electrolyte the capacitance has a maximum close to the immersion potential. This maximum is due to pseudocapacitance probably arising from quinon type surface functional groups as was also observed for activated glassy carbon electrodes [13]. As a consequence the capacitance of a respective device will be smallest in the charged state and largest in the discharged state. The result obtained for H_2SO_4

is not general for aqueous electrolytes. In neutral NaClO_4 a butterfly shaped CV is obtained again.

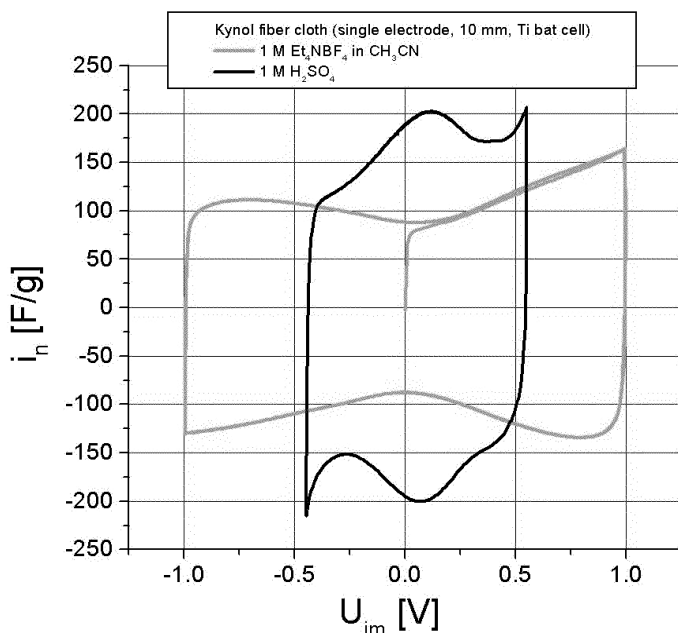


Fig. 8 Cyclic voltammogram of AC Fiber cloth (Kynol) in organic (1 M Et_4NBF_4 in CH_3CN) and aqueous (1 M H_2SO_4) electrolyte. Current normalized to scan rate (10 mV/s) and electrode mass.

As an alternative to acetonitrile-based organic electrolytes for capacitor devices propylene carbonate (PC) is often mentioned. We therefore also studied the behavior in PC electrolyte and found that the results are well in agreement with those observed for AN based electrolyte.

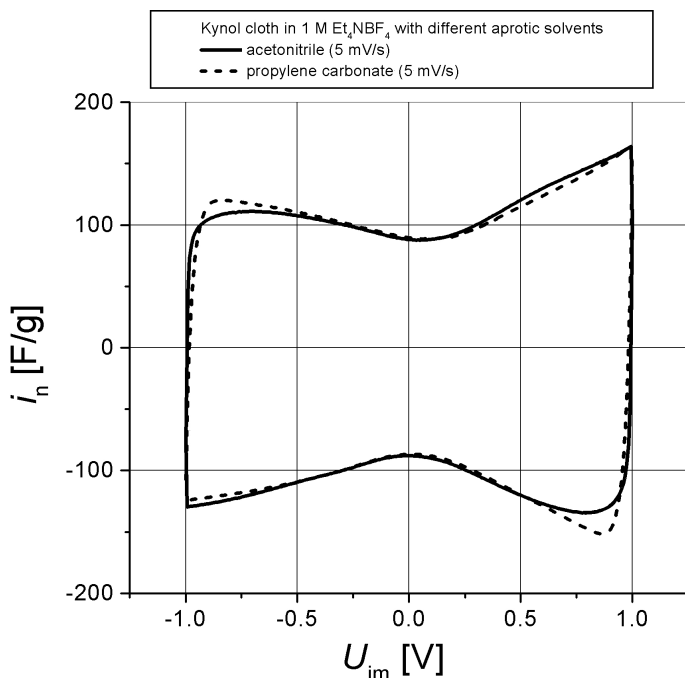


Fig. 9 Cyclic voltammogram of a Kynol cloth electrode in Propylene carbonate (PC) and acetonitrile (AN) based electrolyte.

Figure 9 shows the results for AC Fiber cloth (Kynol) electrode in both AN and PC based electrolytes. Obviously the dependence $C(U)$ is very similar for both solvents.

There are several consequences of the above considerations for optimization and performance of double layer capacitors.

First of all the capacitance per square centimeter is not necessarily determined by the solution side of the double layer and assumptions for the specific capacitance to be 20 or 30 $\mu\text{F}/\text{cm}^2$ are most probably too high. Estimations for the correlation of BET surface area and electrode capacitance usually result in rather low values for the specific capacitance. Such results often lead to the conclusion that not all pores of the AC electrode are utilized. The limited screening ability of the carbon pore walls resulting in a small space charge capacitance, which dominates the overall interface capacitance, may be an alternative explanation.

In order to increase the specific capacitance one should not only think about the solution side of the interface but also about increasing the charge screening capabilities of the respective carbon. It is clear that the density of states should be as high as possible in order to increase the space charge capacitance, which eventually will be dominated by the Helmholtz capacitance.

Secondly, for very high surface area activated carbons it can be estimated that most of the pore walls have a thickness of a few graphene layers only. This is qualitatively demonstrated in Figure 10 where the specific surface area in m^2/g is plotted for a porous structure with slit like pores as a function of the thickness of the walls between pores.

It can be seen that for a surface area of $> 1000 \text{ m}^2/\text{g}$ the walls between pores have thickness $< 1 \text{ nm}$. For 1 nm walls between two pores the effects discussed above may well be important when considering a screening length ($1/e$ value) of about 0.3 nm on both sides. For a surface area $> 2000 \text{ m}^2/\text{g}$ the pore wall thickness approaches the thickness of one graphene layer only. For such walls a significant reduction of the specific capacitance can be expected because the screening capability of the pore wall is now very limited.

For pore walls that thin a situation may arise where the complete screening of the charge is no longer possible, especially when keeping in mind that electrolyte contacts the wall on both sides. The lack of screening will result in reduced capacitance of the carbon material. The potential not screened at the interface will result in an additional potential drop at the back contact of the electrode.

The relatively small capacitance observed for carbon materials with extreme surface areas $> 2000 \text{ m}^2/\text{g}$ by various authors and in our laboratory may be explained by this effect in addition to pore size limitations.

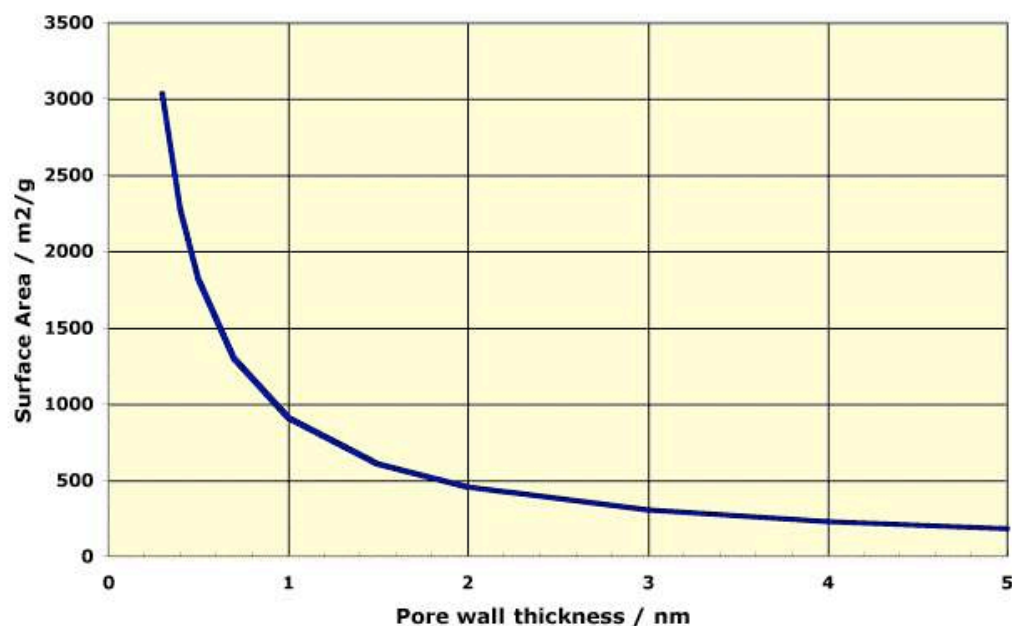


Fig. 10 Specific surface area as a function of pore wall thickness for a porous material assuming slit-like pores and a density of 2.2 g/cm^3 for the bulk wall material.

Thirdly, the potential dependence of the capacitance (butterfly shape of the CV) is rather fortunate for EDLC applications. The capacitance is largest in the charged state where the capacitor will work most of the time. For aqueous carbon based capacitors the contribution of surface functional groups results in a maximum capacitance in the discharged state [13,14], which is not very beneficial. Furthermore, with respect to voltage balancing issues of capacitor chains the increase of capacitance with voltage dilutes the voltage run-away of capacitors with lower capacitance.

Acknowledgement

Financial support of this work by the Swiss CTI (project # 5807.2 KTS-NM, and # 5945.2 TNS) and by Maxwell Technologies SA, Rossens (Switzerland) is gratefully acknowledged. Maxwell Technologies SA and TIMCAL SA, Bodio (Switzerland) provided the capacitor and activated carbon powder, respectively.

References

- ¹ H. Shi, *Activated carbons and double layer capacitance*, *Electrochimica Acta* **41** (1996) 1633.

-
- ² G. Salitra, A. Soffer, L. Eliad, Y. Cohen, D. Aurbach, *Carbon electrodes for double-layer Capacitors, I. Relations between Ion and Pore Diameter*, J. Electrochem. Soc. **147** (2000) 2486.
- ³ K. Kinoshita, *Carbon, Electrochemical and Physicochemical Properties*, Wiley, New York (1987).
- ⁴ I. Tanahashi, A. Yoshida, A. Nishino, J. Electrochem. Soc., **137** (1990) 3052.
- ⁵ G. Salitra, A. Soffer, L. Eliad, Y. Cohen, D. Aurbach, J. Electrochem. Soc., **147** (2000) 2486.
- ⁶ M. Hahn, M. Baertschi, O. Barbieri, J-C. Sauter, R. Kötz, R. Gallay, *Interfacial Capacitance and Electronic Conductance of Activated Carbon Double-Layer Electrodes*, Electrochemical and Solid State Letters, accepted for publication.
- ⁷ N.F. Mott, E.A. Davis, *Electronic Processes in Non-Crystalline Materials*, 2nd ed., Clarendon Press, Oxford (1979).
- ⁸ J. P. Randin, E. Yeager, *Differential Capacitance Study of Stress-Annealed Pyrolytic Graphite Electrodes*, J. Electrochem. Soc., **118** (1971) 711.
- ⁹ J. P. Randin, E. Yeager, *Differential Capacitance Study on Basal Plane of Stress-Annealed Pyrolytic-Graphite*, J. Electroanal. Chem., **36** (1972) 257.
- ¹⁰ H. Gerischer, *An Interpretation of the Double-Layer Capacity of Graphite-Electrodes in Relation to the Density of States at the Fermi Level*, J. Phys. Chem., **89** (1985) 4249.
- ¹¹ H. Gerischer, R. McIntyre, D. Scherson, W. Storck, *Density of the Electronic States of Graphite - Derivation from Differential Capacitance Measurements*, J. Phys. Chem., **91** (1987) 1930.
- ¹² R.C. Tatar, S. Rabii, *Electronic Properties of Graphite - A Unified Theoretical-Study*, Phys. Rev. B, **25** (1982) 4126.
- ¹³ M.G. Sullivan, R. Kötz, O. Haas, *Thick Active Layers of Electrochemically Modified Glassy Carbon. Electrochemical Impedance Studies*. J. Electrochem. Soc., **147** (2000) 308-317
- ¹⁴ M. Baertsch, R. Koetz, A. Braun, O. Haas, *High Power Electrochemical Double-Layer Capacitor*, Proceedings of the 38th Power Sources Conference (1998) p. 17